



Landward Perspective of Coastal Eutrophication Potential Under Future Climate Change: The Seine River Case (France)

Mélanie Raimonet^{1,2*}, Vincent Thieu¹, Marie Silvestre³, Ludovic Oudin¹,
Christophe Rabouille⁴, Robert Vautard⁴ and Josette Garnier^{1,3}

¹ UMR 7619 Metis, Centre National de la Recherche Scientifique, EPHE, IPSL, Sorbonne Université, Paris, France, ² FR636 IPSL, Centre National de la Recherche Scientifique, Sorbonne Université, Paris, France, ³ FR3020 FIRE, Centre National de la Recherche Scientifique, Sorbonne Université, Paris, France, ⁴ Laboratoire des Sciences du Climat et de l'Environnement, UMR CEA-Centre National de la Recherche Scientifique-UVSQ 8212 et IPSL, Gif-sur-Yvette, France

OPEN ACCESS

Edited by:

Alexandra Pavlidou,
Hellenic Centre for Marine Research,
Greece

Reviewed by:

Francisc Peters,
Institut de Ciències del Mar (CSIC),
Spain
Wei-dong Zhai,
Shandong University, China

*Correspondence:

Mélanie Raimonet
melanie.raimonet@upmc.fr
orcid.org/0000-0001-5953-3950

Specialty section:

This article was submitted to
Marine Biogeochemistry,
a section of the journal
Frontiers in Marine Science

Received: 17 November 2017

Accepted: 05 April 2018

Published: 15 May 2018

Citation:

Raimonet M, Thieu V, Silvestre M,
Oudin L, Rabouille C, Vautard R and
Garnier J (2018) Landward
Perspective of Coastal Eutrophication
Potential Under Future Climate
Change: The Seine River Case
(France). *Front. Mar. Sci.* 5:136.
doi: 10.3389/fmars.2018.00136

Studies quantifying the impact of climate change have so far mostly examined atmospheric variables, and few are evaluating the cascade of aquatic impacts that will occur along the land–ocean continuum until the ultimate impacts on coastal eutrophication potential. In this study, a new hydro-biogeochemical modeling chain has been developed, based on the coupling of the generic pyNuts-Riverstrahler biogeochemical model and the GR4J-CEMANEIGE hydrological model, and applied to the Seine River basin (France). Averaged responses of biogeochemical variables to climate-induced hydrological changes were assessed using climate forcing based on 12 projections of precipitation and temperature (BC-CORDEX) for the stabilization (RCP 4.5) and the increasing (RCP 8.5) CO₂ emission scenarios. Beyond the amount of nutrients delivered to the sea, we calculated the indicator of coastal eutrophication potential (ICEP). The models run with the RCP4.5 stabilization scenario show low variations in hydrological regimes and water quality, while five of the six models run with the increasing CO₂ emissions scenario (RCP8.5) leads to more intense extreme streamflow (i.e., higher maximum flows, lower and longer minimum flows), resulting in the degradation of water quality. For the driest RCP 8.5 projection, median biogeochemical impacts induced by decreasing discharge (until $-270 \text{ m}^3 \text{ s}^{-1}$ in average) are mostly located downstream of major wastewater treatment plants. During spring bloom, e.g., in May, the associated higher residence time leads to an increase of phytoplankton biomass (+31% in average), with a simultaneous -23% decrease of silicic acid, followed downstream by a -9% decrease of oxygen. Later during low flow, major increases in nitrate and phosphate concentrations (until +19% and +32% in average) are expected. For all considered scenarios, high ICEP values (above zero) lasted, indicating that coastal eutrophication is not expected to decrease with changing hydrological conditions in the future. Maximum values are even expected to be higher some years. This study deliberately evaluates the

impact of modified hydrology on biogeochemistry without considering the simultaneous alteration of water temperatures, in order to disentangle the causes of climate change-induced impact. It will serve as a first comparative step toward a more complete modeling experiment of climate change impacts on aquatic systems.

Keywords: climate change, hydro-ecological modeling, nutrients, coastal eutrophication potential, impacts

INTRODUCTION

Both urban releases and fertilizer spreading have increased and unbalanced river nutrient fluxes leading to coastal eutrophication in many regions of the world (Nixon, 1995; Billen et al., 1999; Cloern, 2001; Diaz and Rosenberg, 2008; Erismann et al., 2013). Coastal eutrophication has been associated with direct responses, e.g., changes in primary production, nutrient ratios, phytoplankton community, as well as indirect responses, e.g., changes in food web structure, anoxia and fish/invertebrate mortality (Cloern, 2001). These environmental disturbances are highly problematic and environmental management strategies leading to lower nutrient loads and equilibrated N:P:Si ratios are still needed (Billen and Garnier, 1997; Conley et al., 2009).

If we consider the boundaries defining the safe operating space for humanity on Earth proposed by Rockström et al. (2009), i.e., where the Earth system is inside the stable environmental state of the Holocene, human activities have largely exceeded these boundaries for the nitrogen cycle, as well as for climate change, with increasing risks for irreversible climate change situations. Boundaries for nutrient cycles and climate change are not isolated from each other but rather interlinked. For example, the biogeochemical cycle of nitrogen is involved in climate change through the emission of greenhouse gas N_2O , and conversely, changing climate with increasing floods could increase N leaching and N fluxes to the coastal zone. It is therefore essential to evaluate to what extent climate change will have an impact on nutrient cycles (namely nitrogen, phosphorus and silicon) along aquatic continuums and on coastal eutrophication potential.

Recent studies suggest that major impacts of climate change are expected to modify the functioning of marine systems (Doney, 2010; Henson et al., 2016), e.g., an increase in green tides (Gao et al., 2017) and toxic cyanobacteria blooms (Paerl and Paul, 2012; Wood et al., 2017). Many examples suggest that climate change will exacerbate eutrophication symptoms caused by direct anthropogenic activities at the coasts and in the river watersheds, e.g., larger dead zones (Justić et al., 2005; Altieri and Gedan, 2015), increasing DOC export during winter (Huntington et al., 2016), higher nitrate export (Bouraoui et al., 2004), resulting in unbalanced nutrient ratios with respect to P and Si. Other case studies showed an attenuation of these symptoms associated with climate change, e.g., a decrease in nitrate export (Bussi et al., 2017).

The main factors explaining these climate-induced changes are modifications in hydrological regimes (e.g., a flow increase in winter, a flow decrease in summer, an increase in the intensity and frequency of extreme events) and a water temperature increase. However, the induced climate change impacts on coastal

eutrophication are not linear but rather complex, as shown by its possible opposite responses to a similar perturbation on different sites, e.g., an increase in eutrophic conditions during wetter periods in the Northern Gulf of Mexico but a decrease in the Hudson River (Justić et al., 2005). Part of this complexity could be explained by the cascade of indirect impacts that occur along the land–ocean continuum (Billen et al., 2009), which is rarely accounted for. Most particularly, it is essential to include the representation of reaction-transport processes occurring in aquatic systems indirectly impacted by climate change through a modification of hydrological conditions.

Few studies have investigated the indirect impacts of climate change on nutrient transfers and they were generally based on small catchments (Bouraoui et al., 2004; Andersen et al., 2006; Wilby et al., 2006; Bussi et al., 2017), rarely expanded to the regional scale. Some authors investigated the combined effects of modified hydrology and water temperature, e.g., in the Elbe River basin (Hesse and Krysanova, 2016), which prevented disentangling the sole effects of modified hydrology. In addition, the impacts have usually been evaluated on total annual fluxes (e.g., N, P, C) at the river outlet, without taking into account the seasonal variability of impacts on multiple nutrient forms from the head stream waters to the major tributaries (or main streams).

The main hypothesis of this study was that eutrophication problems could worsen in the future because of the cascade of impacts caused by climate-induced hydrological changes. The aim was thus to evaluate the indirect impacts of climate change, through the modification of hydrological regimes, on river water quality along the regional Seine hydrosystem (France) and at its outlet at the seasonal scale. We implemented a new hydro-biogeochemical modeling chain, based on the coupling of a spatialized version of the hydrological GR4J-CEMANEIGE model (Raimonet et al., 2017b) and the biogeochemical pyNuts-Riverstrahler model (www.fire.upmc.fr/rive; Desmit et al., 2015). This allowed evaluating the spatial and temporal impacts of modified hydrology on multiple biogeochemical cycles simultaneously (N, P, Si, C) for a large river basin with strong anthropogenic inputs. We also used an Indicator of Coastal Eutrophication Potential (ICEP) (Billen and Garnier, 2007) to evaluate the modification of coastal eutrophication potential under climate-induced hydrological changes in the future. The sensitivity of the response of biogeochemical variables was assessed using three GCMs, five RCMs and two prospective situations for the timeline 2100: (i) the RCP 8.5 extreme IPCC scenario and (ii) the RCP 4.5 stabilization scenario.

METHODS

The Seine River Basin

Located in northern France, the Seine River is a seventh-order stream at the chosen resolution of the study (**Figure 1**) and is the second longest French river (776 km; 22,400 km cumulated). The Seine River basin drains a surface of 75,989 km² (65,586 km² at Poses) characterized by intense anthropogenic pressures. Intensive agriculture is largely present, mostly in the central part of the basin (Billen et al., 2007), leading to high nitrate water contamination and eutrophication symptoms in the downstream coastal waters (Passy et al., 2016). The population density is high (~220 inhabitants.km⁻² in 2016) with 12 million inhabitants concentrated in the Paris conurbation on only 16% of the basin's surface area. The elevation is homogeneous, with less than 1% of the catchment above 550 m, and the climate is temperate with oceanic influences.

The Hydro-Biogeochemical Modeling Approach

The modeling chain is based on the coupling of the GR4J-CEMANEIGE hydrological model and the pyNuts-Riverstrahler biogeochemical model through 10-day water runoff at the scale of unitary catchments covering ~10 km².

The GR4J-CEMANEIGE Hydrological Model

A semi-distributed hydrological model was set up to estimate daily water surface flow and baseflow on 5,793 catchment units, from daily climate forcing.

The hydrological model needs three climate variables as inputs: air temperature, precipitation, and potential evapotranspiration, which were extracted at the catchment scale and at a daily time step. In this study, the hydrological model GR4J (Perrin et al., 2003) was coupled with the CEMANEIGE snow-accounting module (Valéry et al., 2010) since snowfall may occur within the upstream part of the catchment (see Raimonet et al., 2017b for further detail on the description of the coupling). This model was chosen because it provides relatively good performance (e.g., Perrin et al., 2003) and is commonly used by operational services for hydrological predictions in France.

Since the majority of the 5793 CCM catchments were ungauged, i.e., no flow data were available to calibrate the GR4J model parameters, we used the model parameters calibrated on the gauged catchments ($n = 349$) in the vicinity of each ungauged catchment (Oudin et al., 2008). To apply this approach, we determined the total upstream catchment areas, i.e., the area draining to the CCM unit outlet, and computed streamflow using the GR4J-CEMANEIGE hydrological model. Surface flow and baseflow contributions were then estimated using the BFLOW automatic hydrograph separation method (Arnold and Allen, 1999). Finally, 10-day runoff values (combining surface flow and baseflow) were distributed in each CCM catchment from upstream to downstream, by computing the difference between the drained catchment flows and the flows from smaller nested catchments.

The pyNuts-Riverstrahler Biogeochemical Model

The Riverstrahler model describes benthic and pelagic biogeochemical processes along the river network, from headwater streams to large tributaries (Billen et al., 1994, 2007; Garnier et al., 1995, 2002). It enables a fine-scale representation of the whole drainage network, either by sub-basins, assuming an average functioning by Strahler (1957) stream order, or with a more detailed representation of river branches, kilometer by kilometer. Briefly, Strahler orders are distributed between the first-order streams located upstream of the catchment (order 1) and the largest-order stream that reaches the outlet (order 7). The model takes into account the dynamics of silicified (i.e., diatoms) and nonsilicified phytoplankton and zooplankton and simulates the biogeochemical cycles of carbon, oxygen, nitrogen, phosphorus and silica (under different forms). Most of the processes that are important in the transformation and/or retention of nutrients during their transfer in streams are explicitly calculated at a time step smaller than 6 min and the model outputs are provided at a 10-day resolution.

The pyNuts modeling environment aimed at enabling a large-scale deployment of the Riverstrahler modeling approach to multiple regional river basins (www.fire.upmc.fr/rive). Setting up the pyNuts-Riverstrahler model required to gather different constraints, corresponding namely to morphological properties of the hydrosystems (depth, width, and length), point sources (e.g., wastewater treatment plants), diffusive sources (e.g., agriculture) and hydro-climatic inputs (light, water temperature and runoff).

Setting Up the Modeling Chain Natural Constraints

The pan-European CCM catchment database v2.1 (Vogt et al., 2007; <http://ccm.jrc.ec.europa.eu>) was used to define elementary catchments (5,793 units) for the Seine basin and basic morphological information for characterizing the drainage network. The light followed an annual cycle dependent on the latitude of the catchment, and water temperature was set by Strahler order (adapted from Billen et al., 1994).

Anthropogenic Constraints

Domestic point sources were set from the European UWWTD waterbase (EEA, 2012) using data reported for the year 2010. Fluxes of N, P, C and suspended solids discharged to the drainage network were calculated on the basis of a spatially explicit census of wastewater treatment plants. For each release point, raw emissions were provided (in inhabitant equivalents), associated with a wastewater treatment type (including discharge without any treatment). The corresponding water and nutrient fluxes were considered constant over the year.

Diffuse sources were estimated for surface runoff and base flow as nutrient concentrations characterizing each land use class of the watershed. Data were retrieved from European databases and regionalized for each land use class (Bossard et al., 2000; EEA, 2007; Corine Land Cover database) inside each statistical NUTS region (NUTS level 3). Particulate sources were estimated from the PESERA model (Kirkby et al., 2004) combined with land-based estimates

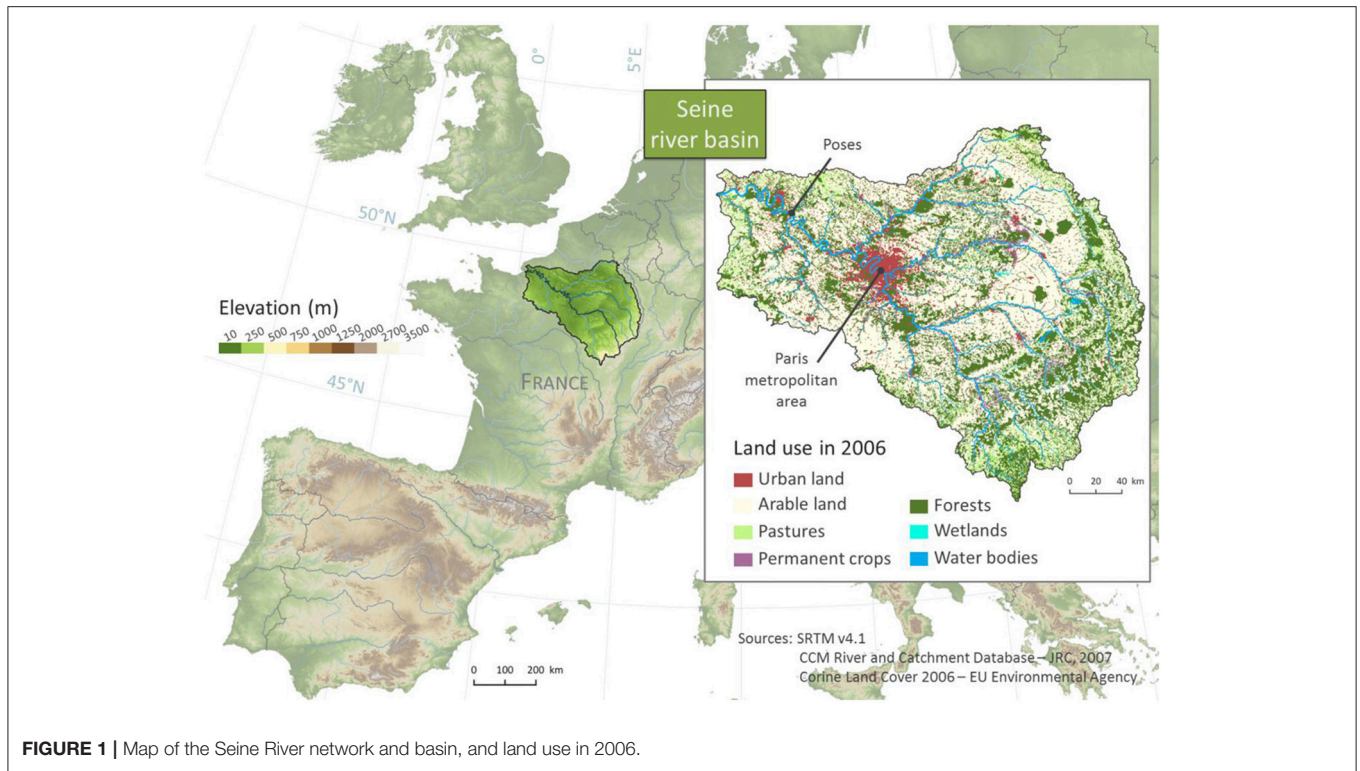


FIGURE 1 | Map of the Seine River network and basin, and land use in 2006.

of phosphorus and organic carbon (LUCAS survey; Tóth et al., 2013). Dissolved silica concentrations were determined according to litho-morphological properties, distinguishing crystalline and sedimentary rocks. Nitrogen (nitrate) leaching flux was calculated based on a comprehensive analysis of the agricultural EUROSTAT databases and N surplus (Anglade et al., 2015) established with the GRAFS (generalized representation of agro-food systems) approach (Billen et al., 2014).

Given that the objective of this work was to evaluate the impact of climate-induced changes, human practices (i.e., domestic point sources and agricultural diffuse sources) were set to conditions characteristic of 2010 and 2006, and kept constant in future scenarios.

Climate Forcing: Reanalyses and Projections

We used the MESAN reanalyses of air temperature and precipitation at a daily timescale (Landelius et al., 2016), as atmospheric inputs for the recent period (2000–2010). Potential evapotranspiration was calculated from the mean daily air temperature and latitude of the catchment using an empirical temperature-based formula (Oudin et al., 2005). MESAN reanalyses were selected for two reasons: these reanalyses used a high-density network of precipitation and temperature observations, making them reliable inputs to the hydrological model (Raimonet et al., 2017b) and the resolution of the MESAN grid was relatively high and similar to the EURO-CORDEX grid (~12 km; <http://www.euro-cordex.net/>; Jacob et al., 2014) on which the climate projections

were downscaled at the European scale. The European scale of the reanalyses and projections was essential because the objective of the pyNuts-Riverstrahler platform, including the new developments presented in this paper, is to extend investigations of climate-induced changes on the West European domain.

For prospective simulations, we used climate model outputs from the bias-corrected version of the EURO-CORDEX projections (BC-CORDEX; see for example, Casanueva et al., 2016). These products were specific to Europe and downscaled to a much higher resolution (12 km) compared to CMIP projections (50 km). We used the BC-CORDEX projections that were corrected for bias using the MESAN reanalyses and the cumulative distribution function (CDF-t; Vrac et al., 2012) with specific processing of precipitation (Vrac et al., 2016). More specifically, we used 12 climate projections (**Table 1**) obtained from a partial combination of three global climate models (GCMs), five regional climate models (RCMs) and two prospective scenarios of CO₂ emissions for the 2100 timeline, i.e., the RCP 8.5 extreme IPCC scenario (+8.5 W/m² in 2100 compared to the preindustrial values) and the RCP 4.5 stabilization scenario (+4.5 W/m²). Each climate simulation covered the 1951–2100 period at a daily timescale.

Note that, in this paper, the term “projection” refers to any combination of global climate model/regional climate model/CO₂ emission scenario leading to one climate situation, while “scenario” refers to the RCP8.5 or RCP4.5 CO₂ emission scenarios, which could include several projections.

TABLE 1 | List of GCM, RCP and RCM combinations used in this study, as well as the climate variable (precipitation P, temperature T, potential evapotranspiration E) and associated hydrological variables (Qmean, mean annual 10-day streamflow; Qmin, minimum annual 10-day streamflow; Qmax, maximum annual 10-day streamflow) change trends for the 1952–2100 period.

Code	Institute	GCM	RCP	RCM	P	T	E	Qmean	Qmin	Qmax
ICHEC45_CLMcom	ICHEC	EC-EARTH	4.5	CLMcom-CCLM4-8-17	0	+	+	–	–	0
ICHEC45_DMI	ICHEC	EC-EARTH	4.5	DMI-HIRHAM5	0	+	+	0	–	0
ICHEC45_KNMI	ICHEC	EC-EARTH	4.5	KNMI-RACMO22E	0	+	+	–	–	0
ICHEC85_CLMcom	ICHEC	EC-EARTH	8.5	CLMcom-CCLM4-8-17	–	+	+	–	–	–
ICHEC85_DMI	ICHEC	EC-EARTH	8.5	DMI-HIRHAM5	+	+	+	0	–	0
ICHEC85_KNMI	ICHEC	EC-EARTH	8.5	KNMI-RACMO22E	0	+	+	–	–	0
IPSL45	IPSL	IPSL-CM5A-MR	4.5	IPSL-INERIS-WRF331F	+	+	+	+	0	+
IPSL85	IPSL	IPSL-CM5A-MR	8.5	IPSL-INERIS-WRF331F	+	+	+	+	+	+
MPI45_CLMcom	MPI-M	MPI-ESM-LR	4.5	CLMcom-CCLM4-8-17	0	+	+	0	–	0
MPI45_MPI	MPI-M	MPI-ESM-LR	4.5	MPI-CSC-REMO2009	0	+	+	0	0	0
MPI85_CLMcom	MPI-M	MPI-ESM-LR	8.5	CLMcom-CCLM4-8-17	0	+	+	–	–	0
MPI85_MPI	MPI-M	MPI-ESM-LR	8.5	MPI-CSC-REMO2009	0	+	+	0	–	0

Trends are determined using the Mann-Kendall nonparametric test (0, no significant trend; +, positive trend; –, negative trend) with the significance threshold at 0.05.

Assessment of the Hydro-Biogeochemical Modeling Chain and Model Outputs Under Future Climate Change

The modeling chain simulations were assessed for the 2000–2010 period for hydrology, and for two contrasted years (2001: wet, 2007: dry) for biogeochemistry. The integrative assessment of all biogeochemical variables is presented at Poses, the outlet of the Seine River basin before tidal influence.

Future changes in river biogeochemistry were assessed by comparing the end of the century (2080–2100) to the reference period (1980–2000) for the two IPCC scenarios, RCP4.5 and RCP8.5 (considering an average of six projections for each scenario). A first focus on each individual projection of the RCP 8.5 was provided, to finally conduct a detailed study of the driest projection ICHEC85_CLMcom and the wettest projection IPSL85. We evaluated *temporal impacts* by investigating seasonal variations of a selection of biogeochemical properties in the future compared to the reference, and *spatial impacts* by investigating variations by Strahler stream order.

The total export fluxes of N, P, and Si, and the ICEP indicator (Billen and Garnier, 2007) were estimated at the river outlet. The ICEP indicator is based on these TN, TP, and TSi fluxes and quantifies the unbalanced river nutrient inputs compared to the requirements of diatom growth (Billen and Garnier, 2007). The N-ICEP and P-ICEP indicators were calculated with the following equations when N or P is limiting, respectively:

$$N\text{-ICEP} = [N\text{Flux}/(14 * 16) - Si\text{Flux}/(28 * 20)] * 106 * 12$$

$$P\text{-ICEP} = [P\text{Flux}/31 - Si\text{Flux}/(28 * 20)] * 106 * 12$$

NFlux, *PFlux*, and *SiFlux* fluxes are expressed in kgN km⁻² d⁻¹, kgP km⁻² d⁻¹, and kgSi km⁻² d⁻¹, respectively, and *N-ICEP* and

P-ICEP are in kgC km⁻² d⁻¹. Positive ICEP values indicate a potential for Si limitation for diatom growth and thus for coastal eutrophication.

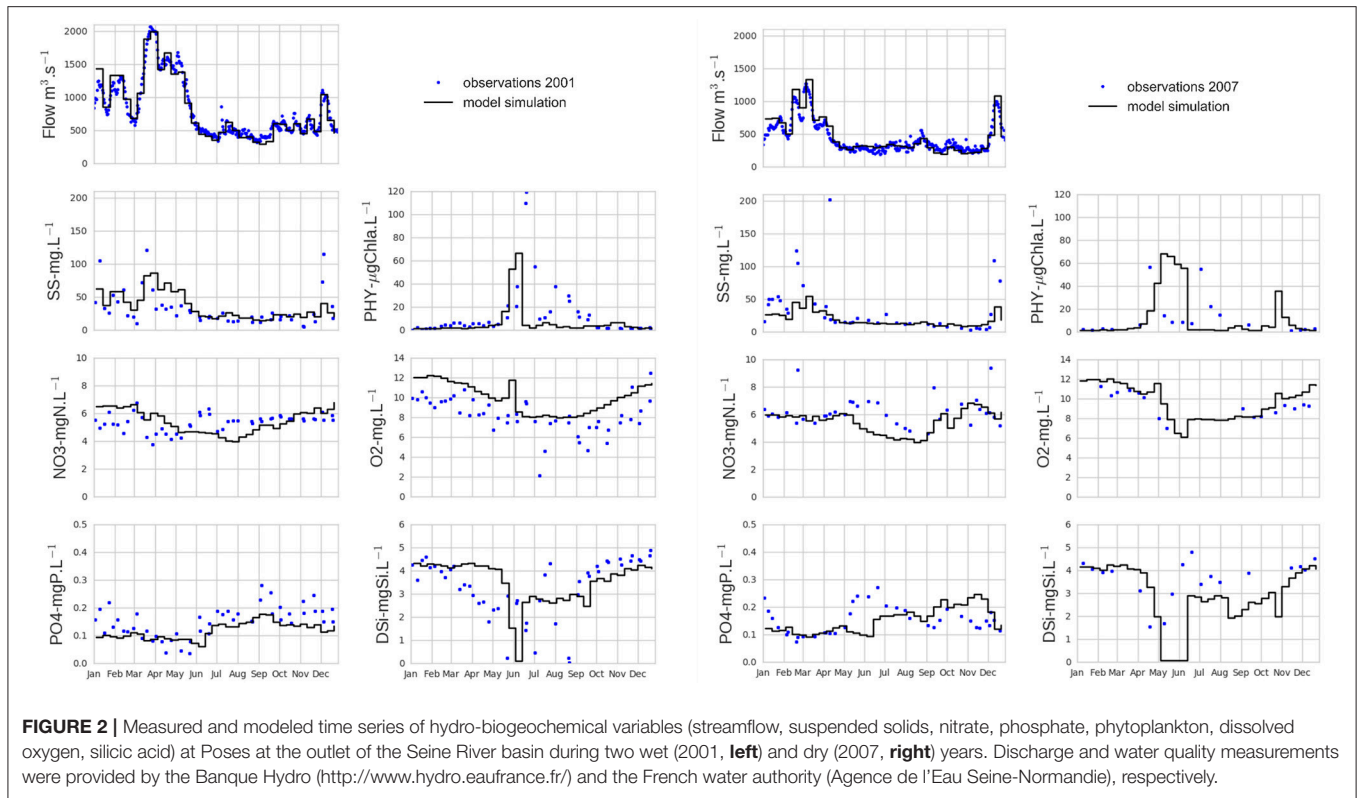
RESULTS

Assessment of the Hydro-Biogeochemical Model Simulations

The spatialized hydrological model developed in this study made it possible to correctly model streamflow at the river outlet (Figure 2) and for catchments nested within the Seine River basin (the simulations on the set of 349 gauged catchments located within the hydrosystem deemed satisfactory, presenting Nash and Sutcliffe (1970) criteria ϵ [0.60 0.99] when the MESAN reanalyses were used as inputs).

Mean streamflow estimations and distributions were generally consistent using MESAN reanalysis and BC-CORDEX projections at the Seine River outlet for the 2000–2010 period (Figure 3), demonstrating the capacity of the hydrological method to estimate past streamflow climatology using climate model outputs. Extreme high flow was accurately represented with most of the climate models, but underestimated with IPSL45 and overestimated with ICHEC45_KNMI.

The model was able to correctly simulate the dynamics of biogeochemical variables (suspended solids, nitrate, phosphate, phytoplankton biomass, dissolved oxygen, silicic acid) for contrasted wet (2001) and dry (2007) situations (Figure 2). Considering that the model is a simplification of reality, the simulations were generally consistent with observations, except some cases where the model outputs were not represented by observations, e.g., underestimation of nitrate between June and August, overestimation of oxygen concentrations in 2001. As an example, the low oxygen concentrations observed in July 2001 must be related to wastewater treatment plant failure and associated releases of high ammonium and/or organic matter concentrations from the 6.5 million equivalent inhabitants



wastewater treatment plant. This type of event has already been highlighted by Aissa-Grouz et al. (2015). As a consequence, low oxygen concentrations has been observed in the data in July 2001. However, this was not simulated by the model, as average wastewater treatment plant loads are used to force the model and not real-time data.

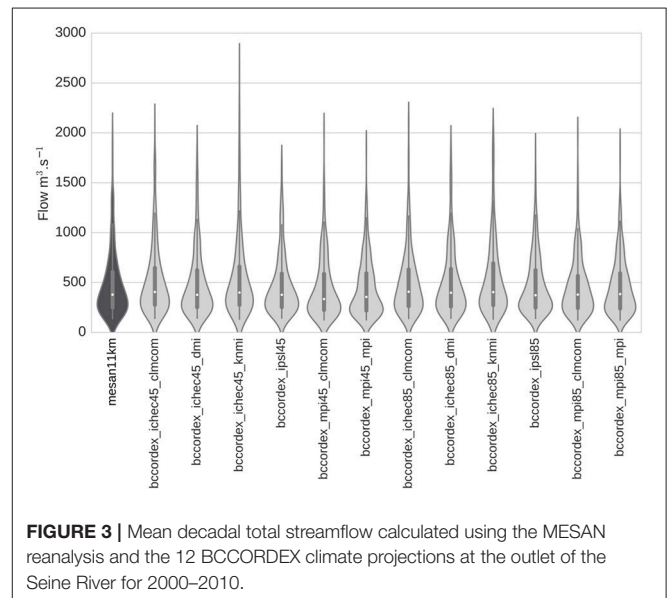
Impacts of Climate Change on Hydro-Biogeochemical Dynamics at the River Outlet

Median Changes for all Climate Projections

Hydrology

Long-term trends of annual climate variables for the Seine River basin (precipitation, air temperature, evapotranspiration) and associated annual hydrological indicators at the basin outlet (average, minimum, and maximum streamflow) were calculated for the 1952–2100 period for each projection (Table 1). Temperature and potential evapotranspiration trends were positive for all projections, while precipitation trends differed depending on projections (eight projections with no significant trend, one with a negative trend, three with a positive trend). This range of climate forcing led to various mean annual streamflow trends (five projections with no significant trend, five with a negative trend, and two with a positive trend). Minimum streamflow trends decreased for nine projections, while maximum streamflow had no trends for nine projections.

Then we compared the changes in hydro-biogeochemical variables at the Seine River outlet between the 1980–2000



reference period and the 2080–2100 future period. When only considering the annual variation in streamflow, we observed a similar 5% increase in streamflow for both RCP4.5 and RCP8.5. However, focusing on seasonal variations indicated that the RCP4.5 stabilization scenario led to lower seasonal hydrological changes compared to the RCP8.5, which resulted in a much stronger modification of hydrological regimes (Figure 4). The

averaged seasonal flow amplitude (between dry and wet seasons) increased from $620 \text{ m}^3 \text{ s}^{-1}$ (reference) to $710 \text{ m}^3 \text{ s}^{-1}$ and up to almost $1,000 \text{ m}^3 \text{ s}^{-1}$ when combining the most extreme averaged values for min-max seasonal RCP8.5 projections. The range of hydrological responses with the six climate projections was wider with the RCP8.5 scenario, indicating that more extreme high and low flows could occur with RCP8.5 compared to the reference and the RCP4.5 scenario. More precisely, extreme flows estimated each year (not shown) covered a wider range of values (from $115 \text{ m}^3 \text{ s}^{-1}$ in summer to $3,250 \text{ m}^3 \text{ s}^{-1}$ during winter) with the scenario RCP8.5 over the period 2080–2100 compared to 1980–2000.

Biogeochemistry

As for hydrology, the RCP4.5 stabilization scenario led to small changes in biogeochemical properties, while the RCP8.5 extreme IPCC scenario led to the greatest changes (see **Figure 4**). Therefore, only the modifications of biogeochemical properties induced by hydrological conditions simulated under RCP8.5 are described hereafter and compared to the reference. Suspended solid concentrations closely followed the changes in streamflow and ranged from $36 \pm 19 \text{ mg l}^{-1}$ in winter to $7 \pm 4 \text{ mg l}^{-1}$ in fall. Compared to the reference period, winter concentrations were higher (median = +14%) and slightly lower in autumn (median = -4%). Nitrate and phosphate concentrations were the most impacted by hydrological changes, and especially by a streamflow decrease in summer/fall. Nitrate and phosphate concentrations increased during this period (from $4.7\text{--}6 \pm 0.6 \text{ mgN l}^{-1}$ to $4.9\text{--}6.8 \pm 0.6 \text{ mgN l}^{-1}$ for nitrate; from $0.18\text{--}0.23 \pm 0.4 \text{ mgP l}^{-1}$ to $0.20\text{--}0.26 \pm 0.4 \text{ mgP l}^{-1}$ for phosphate). The change in streamflow in spring (slight increase for RCP8.5) led to a slight lowering in phytoplankton biomass (to $20\text{--}48 \pm 13 \mu\text{g Chla l}^{-1}$ instead of $35\text{--}56 \pm 12 \mu\text{g Chla l}^{-1}$ in April). The bloom was logically followed by less oxygen depletion compared to the reference situation ($9 \pm 2 \text{ mg l}^{-1}$ instead of $7 \pm 2 \text{ mg l}^{-1}$ in May). Silicic acid concentrations generally inversely followed the changes simulated for phytoplankton bloom dynamics, particularly during the spring and autumn blooms. Silicic acid decreased more slowly with RCP8.5 but was still completely depleted by diatom uptake. The fall bloom was still lower than the spring bloom, but slightly increased with RCP8.5, and oxygen and silicic acid concentrations varied accordingly.

Changes by Climate Projection

Although the changes described above were relatively limited when considering the averaged responses of all the projections merged for a given scenario, more contrasted changes were observed when we investigated the individual seasonal response of each projection for the RCP 8.5 most extreme scenario (**Figure 5**).

For example, only one projection (IPSL85) showed an increase in river discharge (up to $+500 \text{ m}^3 \text{ s}^{-1}$, i.e., +40% in February) and suspended solids (up to $+23 \text{ mg l}^{-1}$, i.e., +45% in February). This is due to the increasing modeled rainfall over the catchment in summer, which is different from the other models. All five of the other projections rather indicated an increase in river discharge and suspended solid concentrations

in winter/spring and a decrease in summer/fall ranging between +20 and -20%, respectively (**Figure 5**). One of the projections (ICHEC85_CLMcom) led to the most drastic decrease in river discharge and suspended solids, especially during fall (up to -35%).

Nitrate and phosphate concentrations were modified during the low-flow season. Except for IPSL85, nitrate and phosphate concentrations increased (up to $+2 \text{ mgN l}^{-1}$ and $+0.12 \text{ mgP l}^{-1}$ with ICHEC85_CLMcom in October) in response to the streamflow decrease.

The increase and decrease in phytoplankton biomass (up to +15 and -22 $\mu\text{g Chla l}^{-1}$ during the fall and spring blooms depending on the projection) occurred with the decrease and increase in river discharge, respectively (**Figure 5**). Dissolved oxygen concentration changes were limited (-2.3 to $+2.1 \text{ mg l}^{-1}$) and restricted to post-bloom periods in spring and fall (**Figure 5**). Silicic acid concentrations varied in response to changes in phytoplankton biomass (mostly diatoms, not shown) in spring and fall.

The above changes are averaged values for each projection for the period 2080–2100 compared to 1980–2000. However, strong inter-annual variability (not shown in the figures) indicated even more extreme values depending on simulated years. For example, for the driest projection ICHEC85_CLMcom, nitrate and phosphate concentrations could lead to an absence of change during some years but reach $+3.5 \text{ mgN l}^{-1}$ and $+0.22 \text{ mgP l}^{-1}$ some other years which could strongly worsen the eutrophic status of the system.

Spatial Impacts of the Modified Hydrology on River Biogeochemistry

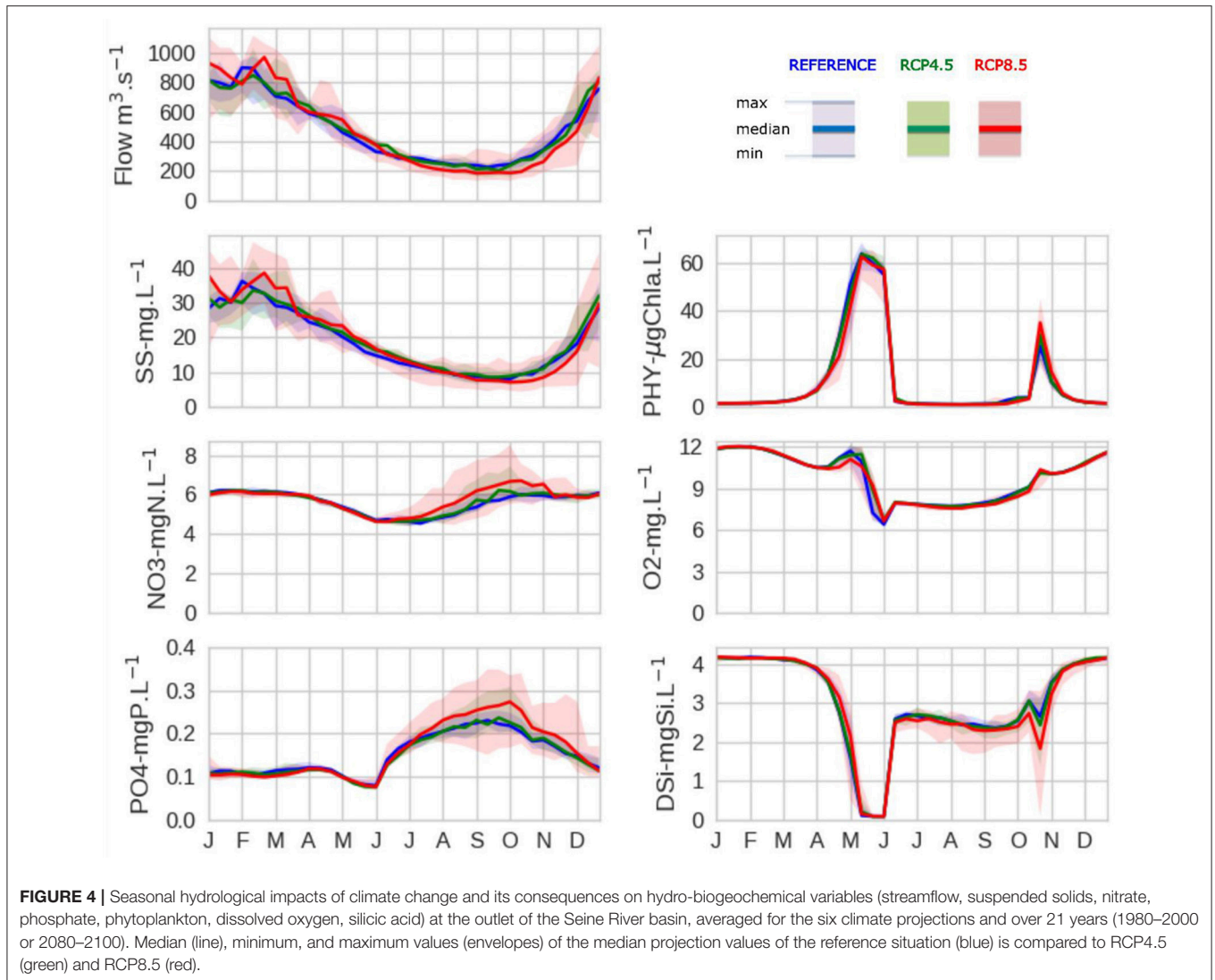
We investigated the spatial impacts of the modified hydrology for the driest projection that led to the lowest streamflow (ICHEC85_CLMcom) during the most sensitive time periods, e.g., during the spring bloom in May and during the late low-flow reduction in October/November (see **Figure 5**). According to Garnier et al. (1995), we only represented Strahler orders starting at 4 where phytoplankton growth rate is higher than dilution by water flow, enabling phytoplankton biomass to increase (**Figures 6, 7**).

During the Spring Bloom in May

Streamflow decreased in the whole hydrosystem, especially for stream orders greater than or equal to 5 (from -10 to $-150 \text{ m}^3 \text{ s}^{-1}$, i.e., $> -20\%$; **Figure 6**). This decrease led to increasing phytoplankton biomass and associated decreasing silicic acid concentrations in these orders and decreasing oxygen concentrations in the 7th order. This is clearly visible along the main Seine River stream (**Figure 8**) where phytoplankton increases and silicic acid decreases mostly occurred between Paris and Poses, followed by an oxygen decrease further downstream toward the estuary.

During the Late Low Flow in October/November

Streamflow strongly decreased in all orders in October/November (almost -50% in all orders and from 360 to $200 \text{ m}^3 \text{ s}^{-1}$ in the 7th stream order; **Figure 7**). This logically led



to a strong decrease in suspended solid concentrations (between -30 and -50%) that reached less than 6 mg l^{-1} in the 7th stream order. This strong decrease in river discharge led to an increase in nitrate and phosphate concentrations in the 7th stream order from 6.2 to 7.3 mgN l^{-1} ($+19\%$; **Figure 7**) and from 0.2 to 0.3 mgP l^{-1} ($+44\%$), respectively. When looking at the distribution along the main Seine River stream (**Figure 8**), the decrease in suspended solid concentrations was intensified downward, while nitrate and phosphate concentrations clearly increased downstream of major wastewater treatment plant effluents.

Changes in Eutrophication Potential to the Coastal Zone

According to the Redfield ratios, both TN and TP fluxes were in excess compared to TSi fluxes at the Seine River outlet for the reference period and hence ICEP indicators were always higher than zero, indicating the sensitivity of this system to coastal eutrophication (**Table 2**), as shown previously (Billen and

Garnier, 2007). When comparing annual export fluxes, a slight increase in TN, TP, and TSi fluxes was observed leading to constant N-ICEP and P-ICEP indicators in the future compared to the reference. However, the largest changes were observed with the wettest projection, IPSL85, and the driest projection, ICHEC85_CLMcom (**Table 2**).

The wettest projection, IPSL85, led to annual increases in TN fluxes (from 3.29 to $3.98 \text{ kg km}^2 \text{ d}^{-1}$), TP fluxes (from 0.11 to $0.13 \text{ kg km}^2 \text{ d}^{-1}$) and TSi fluxes (from 1.52 to $2.08 \text{ kg km}^2 \text{ d}^{-1}$). The driest projection, ICHEC85_CLMcom, resulted in the opposite annual decrease trends in TN fluxes (from 2.93 to $1.87 \text{ kg km}^2 \text{ d}^{-1}$), TP fluxes (from 0.10 to $0.08 \text{ kg km}^2 \text{ d}^{-1}$) and TSi fluxes (from 1.31 to $0.58 \text{ kg km}^2 \text{ d}^{-1}$). In both conditions, N-ICEP remained largely positive, N being in excess to Si; whereas P-ICEP, closer to zero in the wettest condition, showed better balanced P and Si fluxes. For the low-flow period in late summer/fall (August–October), the same trends as for annual values were observed, and N-ICEP and

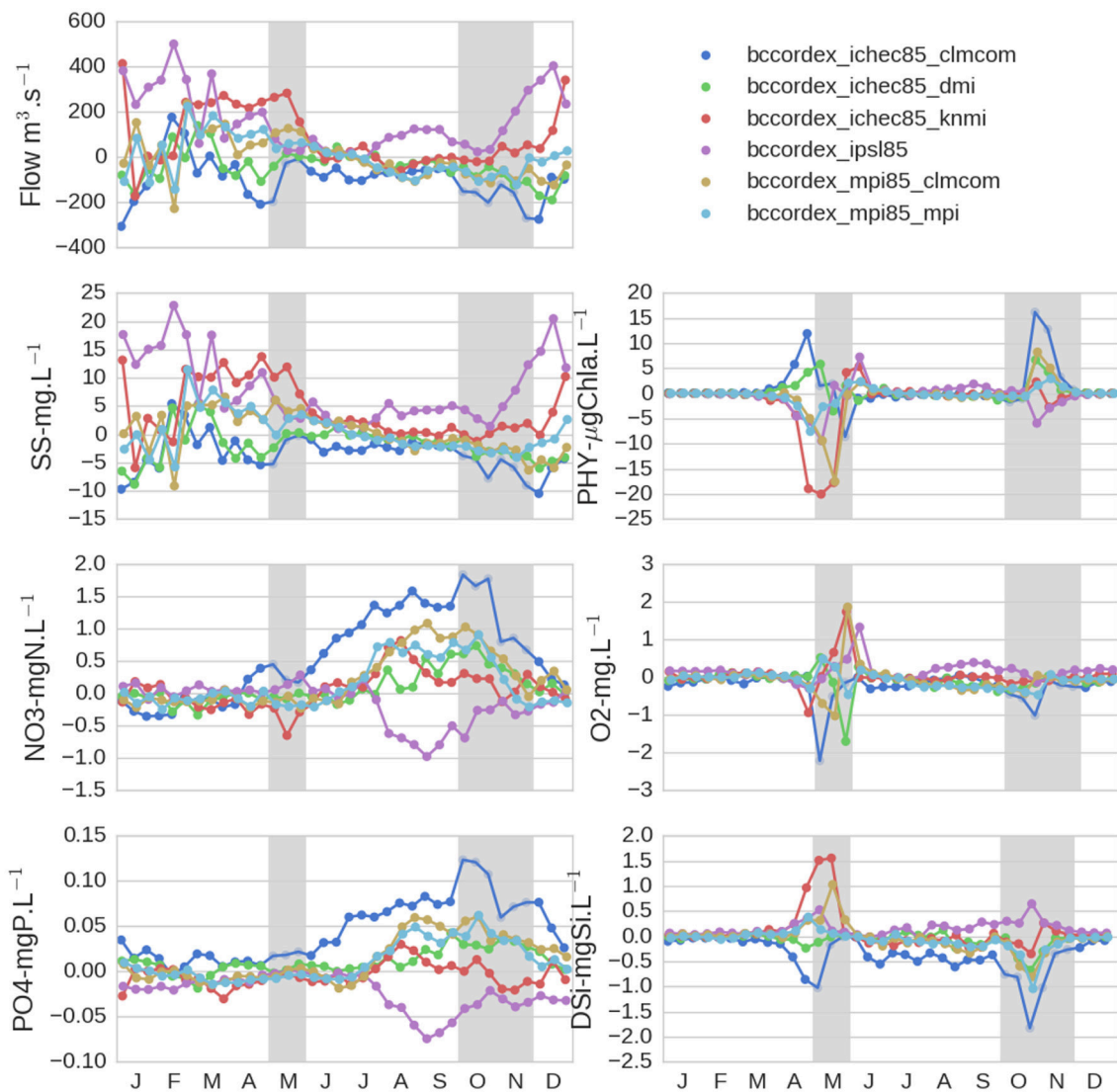


FIGURE 5 | Seasonal impacts of climate change on absolute changes in hydrological and biogeochemical variables at the outlet of the Seine River basin for the six projections of the RCP8.5 scenario. For each projection, absolute changes are the difference between 21-year averages for the 2080–2100 period and for the 1980–2000 reference period. The gray boxes represent periods where spatial impacts were studied in greater detail in **Figures 6, 7**.

P-ICEP indicators remained always above zero, a threshold for coastal eutrophication potential.

Minimum and maximum values of total fluxes and ICEP values indicated that more extreme values are expected in the future compared to the past, for the wettest and driest projections.

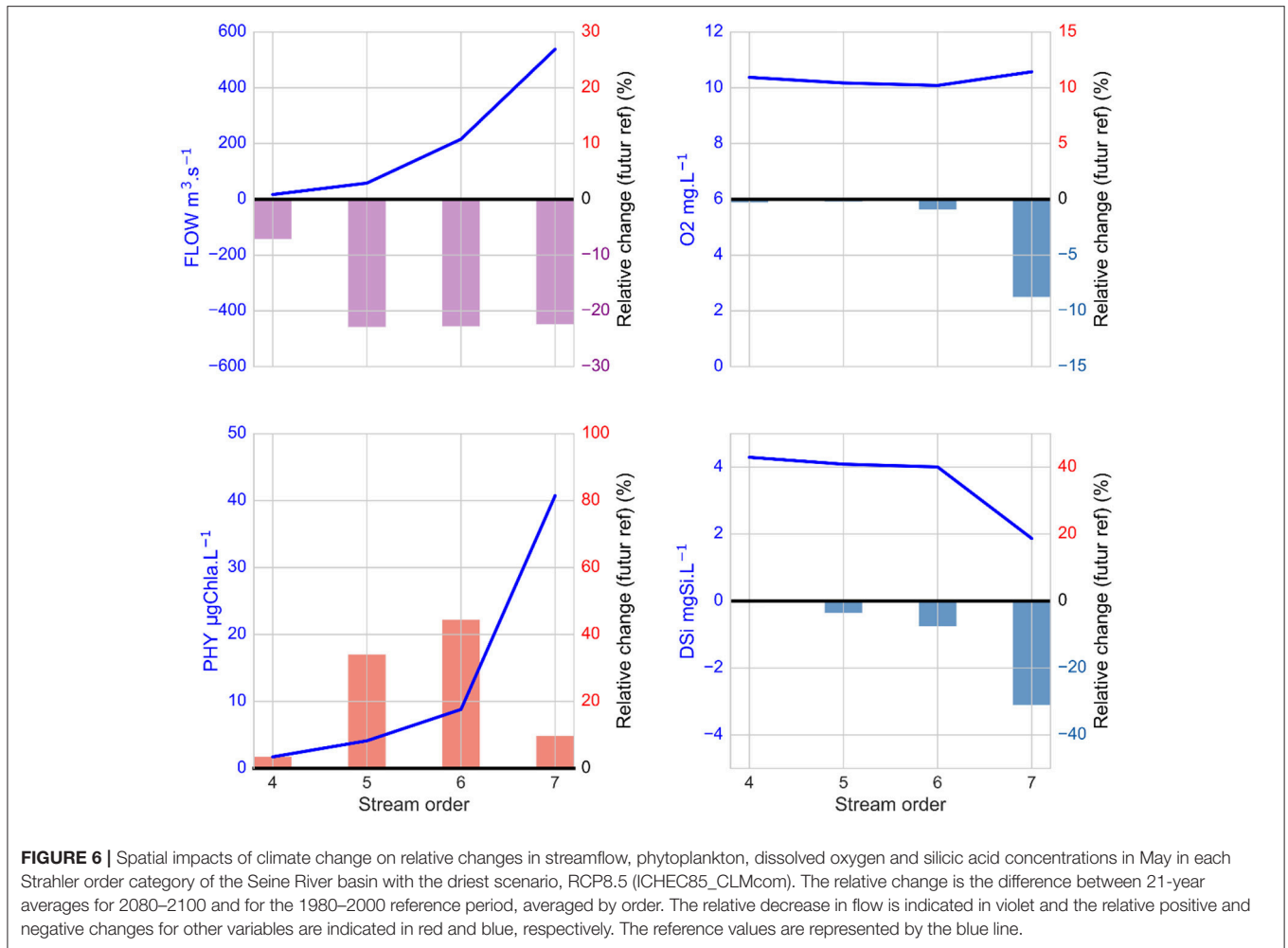
DISCUSSION

Sensitive Seasons to Hydrological Changes and Magnitude of Extreme Events in the Future

From a hydrological and biogeochemical point of view, periods of high flow and low flow are the most sensitive seasons with the

RCP8.5 extreme CO₂ emission scenario. Hydrological regimes are characterized by more contrasted seasons between 2080–2100 and 1980–2000, with larger precipitation and streamflow in winter/spring and more severe low flows in summer/fall at the end of the century. This is consistent with previous findings for the Seine River (Ducharne et al., 2003; Dayon, 2015), while other studies based on different climate projections, emission scenarios, downscaling methods, hydrological model and/or periods studied mostly suggested an overall streamflow decrease (e.g., Boé et al., 2009).

The modifications of the hydrological regime observed with the RCP8.5 scenario have biogeochemical consequences in the Seine River hydro-ecosystem, e.g., (i) an impact on water quality along the hydro-ecosystem through its outlet, as exemplified for spring and fall (see the section on spatial hydro-biogeochemical



impacts) and (ii) an impact on nutrient export and coastal eutrophication potential at the annual scale as well as during low flow (see the section on eutrophication potential to the coastal zone).

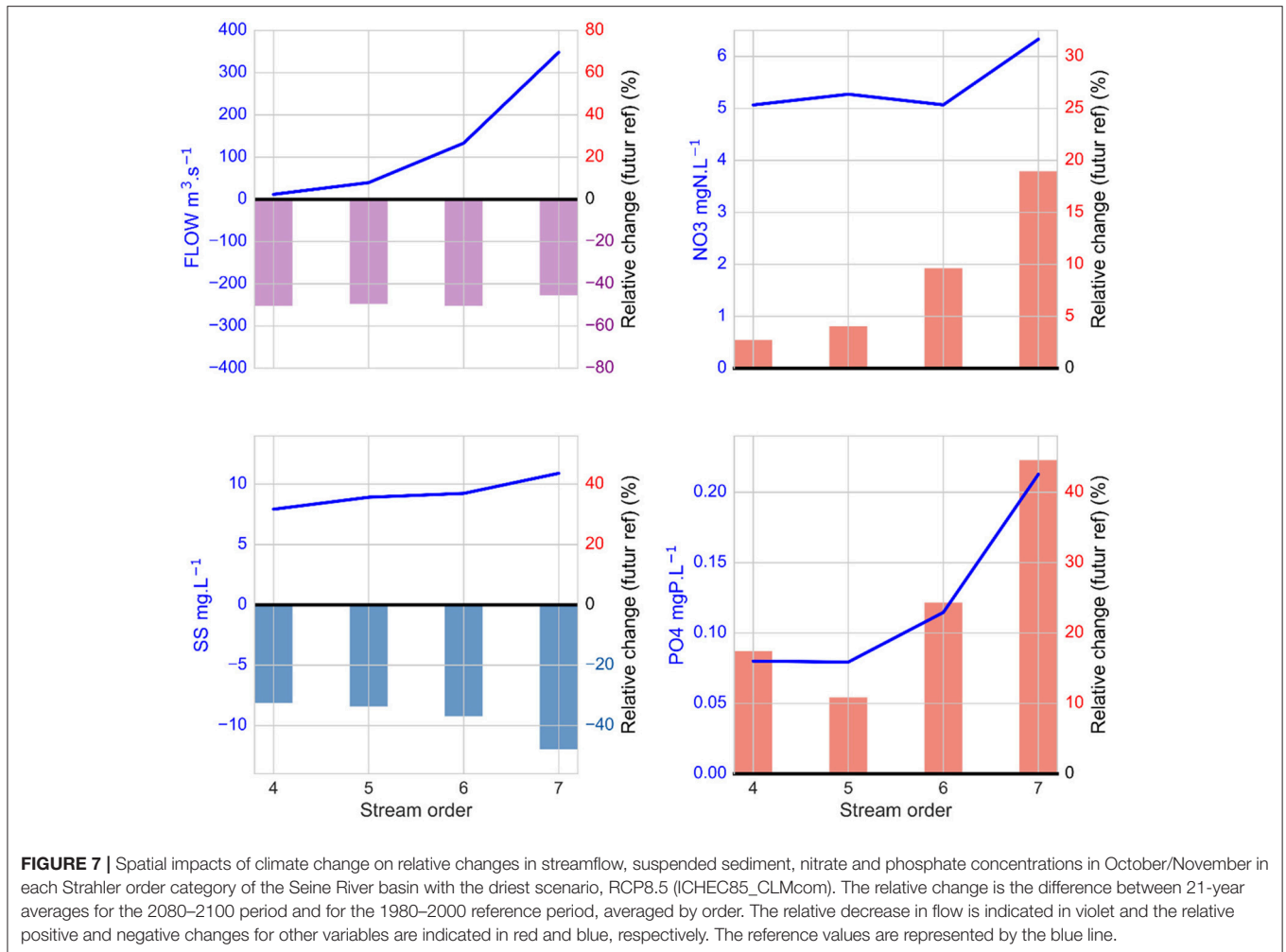
It is worth noting that, even if we do not see drastic changes in median values, there is an increase in the range of values reached with the different climate projections used, particularly the wettest projection, IPSL85, and the driest projection, ICHEC85_CLMcom, indicating that extreme high values in terms of streamflow (floods and droughts) as well as biogeochemical water properties (e.g. coastal eutrophication symptoms) can be expected in the future. These values are even expected to be more extreme due to inter-annual variability with some years exhibiting more extreme minimum or maximum discharge, as well as much higher potential of coastal eutrophication compared to values observed today.

Spatializing Hydro-Biogeochemical Impacts Under Future Climate Change

Part of the originality of this study is to identify how the indirect impacts of climate change (i.e., modified hydrology and its

consequences) are distributed by stream order at the regional scale of the Seine River basin. It is well known that stream orders are characterized by distinct morphology, hydrology and biogeochemical functioning from headwater streams to large rivers downstream (Garnier et al., 1995; Seitzinger et al., 2002; Bouwman et al., 2013). Understanding how the spatial impact of the modified hydrology will alter the river biogeochemistry with climate change is essential in order to detect changes in the spatial distribution of biogeochemical properties by stream order, and to anticipate the combined effects of climate change and anthropogenic pressures.

For the driest climate projection (ICHEC85_CLMcom) during the most sensitive periods in both May and October/November, the streamflow decreases in all stream orders with increasing visible impacts downstream. The biogeochemical modifications occurring with streamflow changes differ depending on the magnitude of hydrological changes, the season and the biogeochemical variable considered. During the productive season, and particularly in May, these changes lead to an increase in the phytoplankton bloom, which grows in the 5–7th stream orders, with increasing residence time. This stimulation of phytoplankton growth (mostly diatoms)

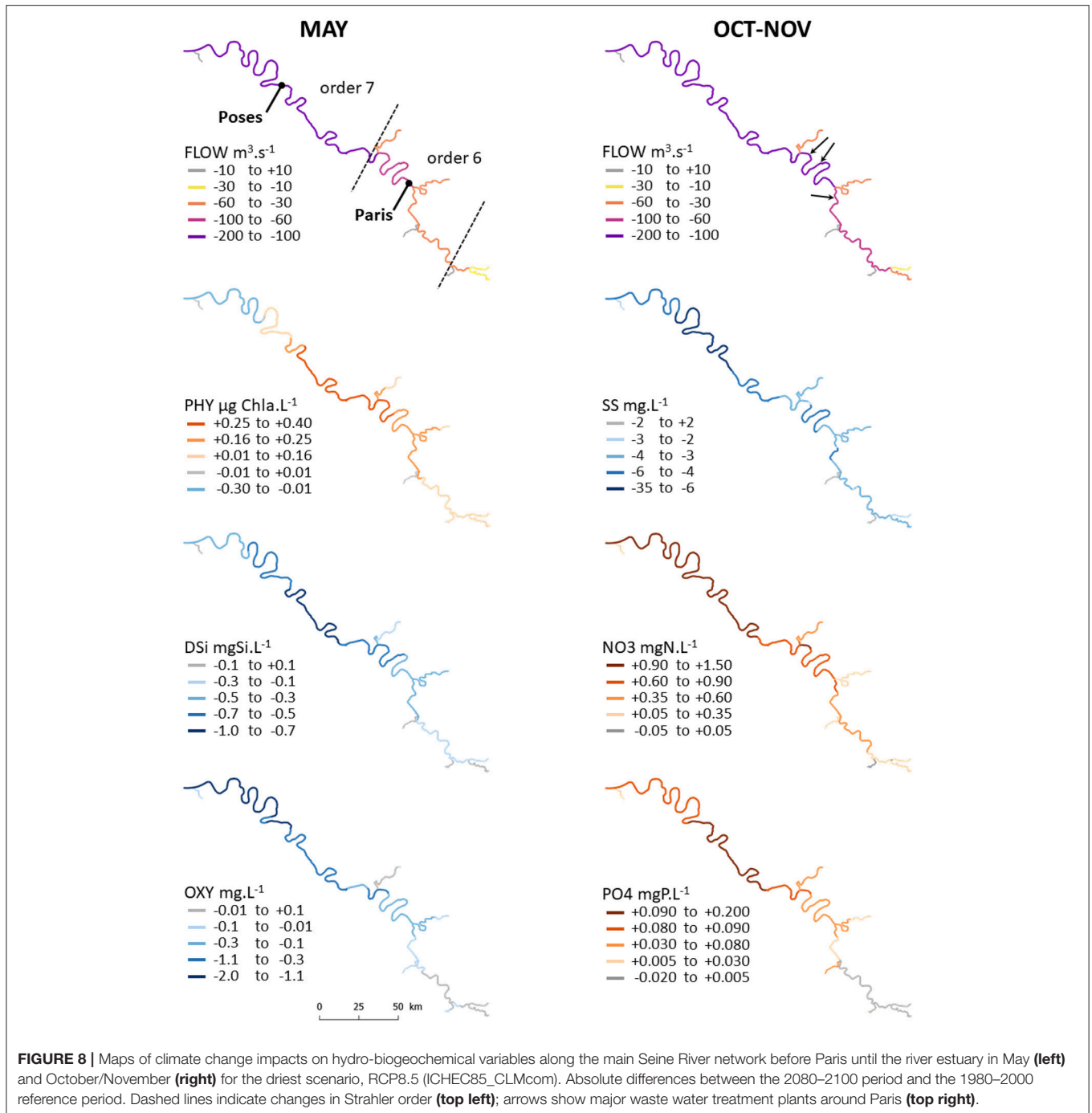


logically leads to a simultaneous silicic acid decrease due to higher silicic acid uptake by diatoms, as well as an oxygen decrease downstream in the 7th stream order, where the phytoplankton biomass is transported to form more abundant organic matter degraded by heterotrophic activities (decreasing oxygen). Under the RCP8.5 extreme CO₂ emission scenario, the maximum of phytoplankton biomass is still located in the 5th orders, but amplifies in these orders and increases farther upstream in the 4th orders. This indicates that phytoplankton grows more upstream in the hydro-ecosystem in response to the streamflow decrease and the associated increase in water residence time. These results highlight that climate-induced hydrological changes will have consequences in terms of amplitude and localization of phytoplankton blooms and associated biogeochemical variables, e.g., oxygen and silicic acid, which are both associated with eutrophication symptoms.

During the low-flow season, when the streamflow decrease is expected to be substantial and extended, suspended solid concentrations strongly decrease due to lower erosion and higher sedimentation in the river. These changes are known to have consequences on geomorphological river properties, phytoplankton growth, contaminant accumulation,

benthic recycling, etc. Simultaneously, nitrate and phosphate concentrations increases during low flow, particularly in the 7th stream order, are most likely related to the lower dilution of point sources in the urbanized river basin, as commonly observed downstream of large sewage treatment plant effluents. In addition, the increase in nitrate is also related to higher nitrification rates resulting from higher ammonium concentrations and higher water residence time, as already observed in the Seine River (Garnier et al., 2007; Aissa-Grouz et al., 2015; Raimonet et al., 2017a). The biogeochemical impacts of river flow decrease are thus expected to be greater downstream of conurbations with major sewage treatment plant effluents.

Suspended matter, oxygen, nitrate, and phosphate concentrations present a similar trend regardless of the stream order considered and the climate projection used, but these impacts are often stronger downstream in higher stream orders (>4th). This result supports the idea that the climate-induced modified hydrology impacts cascade in all stream orders for these biogeochemical variables, with cumulative effects on biogeochemical processes from upstream to downstream. Stronger spatial heterogeneity could be expected in larger river



basins characterized by a diversity of climate regimes inside its watershed as well as in highly impaired river basins.

Interestingly, the absolute increase in nitrate concentrations expected with the driest RCP85 scenario might locally be on the same order of magnitude and even higher than the range of seasonal variability and the spatial variations observed from stream orders 1–7. This means that the amplitude of the biogeochemical impact induced by climate change is, for

example, for nitrate, comparable to the impact of direct anthropic pressures through agriculture and wastewater treatment effluents on the basin, or to the effect of the retention capacity associated with the denitrification biological process. This study demonstrates the adverse impacts on aquatic biogeochemistry and supports the need for decreasing N and P sources to reduce coastal eutrophication symptoms (Billen and Garnier, 1997; Conley et al., 2009).

TABLE 2 | Annual median values for TN, TP and TSi fluxes, and indicators of coastal eutrophication potential (N-ICEP and P-ICEP), for all projections as well as for the wettest (IPSL85) and the driest (ICHEC85_CLMcom) projections.

Projections	Type	Period	RCP	TN (kgN km ⁻² d ⁻¹)	TP (kgP km ⁻² d ⁻¹)	TSi (kgSi km ⁻² d ⁻¹)	N-ICEP (kgC km ⁻² d ⁻¹)	P-ICEP (kgC km ⁻² d ⁻¹)
All		1980/2000	Reference	2.94 [1.71 5.26]	0.10 [0.08 0.15]	1.33 [0.48 3.20]	14.21 [9.66 22.40]	1.05 [−0.98 1.86]
		2080/2100	RCP8.5	2.98 [1.49 4.72]	0.11 [0.07 0.15]	1.36 [0.27 3.17]	14.42 [7.95 20.85]	1.05 [−1.03 2.26]
IPSL85	Wettest	1980/2000	Reference	3.29 [2.08 3.89]	0.11 [0.08 0.12]	1.52 [0.63 2.24]	15.30 [10.42 17.45]	1.00 [−0.48 1.70]
		2080/2100	RCP8.5	3.98 [2.51 4.71]	0.13 [0.09 0.15]	2.08 [0.85 3.00]	17.92 [12.54 20.46]	0.38 [−1.03 1.63]
ICHEC85_CLMcom	Driest	1980/2000	Reference	2.93 [2.12 4.50]	0.10 [0.08 0.14]	1.31 [0.74 2.82]	13.46 [10.20 18.89]	1.08 [−0.48 1.64]
		2080/2100	RCP8.5	1.87 [1.49 3.82]	0.08 [0.07 0.13]	0.58 [0.27 2.27]	9.23 [7.95 16.88]	1.84 [0.56 2.26]

Values are given for the reference period, as well as for the future period (2080/2100) for the extreme CO₂ emission scenarios (RCP8.5). Numbers between brackets indicate minimum and maximum annual values.

Eutrophication Potential to the Coastal Zone Under Future Climate Situations

If we consider median values for the RCP8.5 scenarios (median of six projections for each scenario) for 21 years at the end of the century, the eutrophication potential is expected to remain stable compared to the end of the previous century with unbalanced nutrient ratios.

Investigating impacts during the wettest and driest projections individually allows us to better appraise the evolution of coastal eutrophication potential under changing climate. Logically, total annual nitrogen, phosphorus and silica exports decrease with the driest projection (ICHEC85_CLMcom) and increase with the wettest projection (IPSL85), which is consistent with the change in nutrient diffuse sources contribution while point sources loads are estimated independently from hydrological conditions. Our estimates demonstrate that at the outlet of the Seine River, the imbalance of nitrogen fluxes will remain in a large excess over silica fluxes under future climate situations. These high N-ICEP values tend to increase with the wettest projection and decrease with the driest one, which is in agreement with the prevalence of diffuse nitrogen sources for the agricultural Seine basin. In comparison, the low excess of phosphorus fluxes over silica (P-ICEP close to zero) is further lowered to zero under the wettest projection. Increasing runoff conditions under IPSL85 projection will result in greater exports of silica of diffuse sources, compared to the phosphorous exports, issued from both diffuse and point sources (Garnier et al., 2013).

These results suggest that, for a given river basin, ICEP indicators are expected to increase or decrease in response to the hydrological changes, the N and P proportion in diffuse vs. point sources, and the cascade of impacts on biogeochemical processes in the hydrosystem. The evolution of the coastal eutrophication potential therefore depends on the climate regime, the internal catchment properties, and anthropogenic pressures with possible opposite trends (Romero et al., 2012). Indeed, both streamflow increase and decrease can potentially lead to more sensitivity to eutrophication conditions with respect to either the excess of phosphorus or the excess of nitrogen over silica. In coastal waters of the anthropized Seine basin where nutrient ratios of the delivered fluxes are already imbalanced, the predictions of climate change will not support any decrease of the coastal

eutrophication potential to negative values—except some years where P-ICEP could reach values slightly below zero. This indicates that coastal eutrophication could be a burden in the future, as observed today (Romero et al., 2012; Passy et al., 2016), and shows the need to implement management strategies.

This study does not consider the transitional estuarine zone between the river and the coastal systems, which can, however, modify the expression of eutrophication in coastal waters (Cloern, 2001; Cloern et al., 2016). Modeling the Seine estuary already showed its overall minor role in decreasing −6.8 and −11% of the annual average nitrogen and phosphorus load, respectively, due to substantial modification of its geomorphology (Garnier et al., 2010). Despite a phosphorus reduction up to −40% for a short period in summer, taking into account the estuary in the modeling chain did not remove current eutrophication problems in the Seine Bight (Passy et al., 2016). However, for larger domains, the functioning of the estuarine filter under future climate change could be required. In particular, a modeling chain of the entire land–ocean continuum explicitly representing estuarine zones is clearly lacking (Regnier et al., 2014).

Recommendations for Further Assessment of Climate Change Impacts

This study provides reference values of climate-induced hydrological impacts on biogeochemistry and coastal eutrophication sensitivity for a highly anthropized system. We deliberately investigated the hydrological changes induced by hydrology modifications only. This will serve as a basis for further comparisons with temperature increase impacts and for investigations of coupled effects of scenarios of climate and human management strategies.

Indeed, in addition to the indirect hydrological impacts of climate change, there will also be climate change impacts on increasing water temperature that controls most of biological and biogeochemical reaction rates. For example, increasing temperature is known to modify phytoplankton growth rates (Garnier et al., 1995), nitrification and denitrification rates (Dawson and Murphy, 1972; Laverman et al., 2006, 2007; Benoit et al., 2015), bacterial respiration (Thamdrup et al., 1998) and stimulate silica dissolution (Van Cappellen et al., 2002).

Water warming could superimpose with the effects of changing hydrological regimes, leading to even more phytoplankton biomass during the productive season, with a possible shift in the species composition to more nongrazable and/or harmful algae (e.g., Paerl and Paul, 2012), and lower dissolved oxygen concentrations, as shown in the modeling study of Ducharne (2008). Future hydro-biogeochemical modeling studies at the regional scale should integrate spatialized thermal changes throughout the aquatic system, as developed for example in the Loire River (Bustillo et al., 2014; Beaufort et al., 2016), in order to study the effects of synchronous changes in temperature and hydrology on river water quality.

Here, management strategies are representative of those of the reference period and future adaptation strategies have not yet been accounted for. Beside modified hydrology and temperature increase, associated adaptation management strategies should be considered in future work (e.g., modified agricultural practices and systems, water regulation by reservoirs or water withdrawal, ...). Evaluating the cumulative or attenuating impacts on river water quality is a further challenge in order to limit or decrease coastal eutrophication symptoms, as already stressed in previous studies (e.g., Billen and Garnier, 1997; Rabalais et al., 2009; Romero et al., 2012).

CONCLUSIONS

A spatialized hydrological model has been implemented and coupled to the existing biogeochemical pyNuts-Riverstrahler model. This new hydro-biogeochemical model has been successful in modeling hydro-biogeochemistry in the past-present, and is useful for the modeling of future hydro-biogeochemistry under a changing climate.

Our results showed that the RCP4.5 stabilization scenario resulted in weak variations in hydrological regimes and water quality, suggesting that moderate indirect impacts of climate change are expected if CO₂ emissions are stabilized. However, increasing CO₂ emissions with the business-as-usual scenario (RCP8.5) would lead to more frequent and intense extreme streamflow (i.e., higher winter flow, lower minimum flow, prolonged period of low water flow), leading to the degradation of water quality in addition to floods, droughts, water shortages, etc.

At the river outlet, the streamflow decrease during low flow with RCP8.5 produced modifications of biogeochemical properties (nitrate, phosphate and phytoplankton increases) related to lower point source dilution and higher water residence time, as well as the cascade of modified instream biogeochemical

processes leading to lower silicic acid and oxygen concentrations. The streamflow increase in winter was associated (in most of the climatic projections) with intensified nutrient exports that increase coastal eutrophication potential, which is still expected to be above the threshold of balanced nutrients in the future, regardless of the projection considered.

In addition to impacts at the river outlet, drastic spatial impacts in biogeochemical properties were evidenced under extreme climate projections along the river network. Under the driest climate projection, phytoplankton biomass was expected to increase in 5th and 6th-order streams in May due to increasing residence time, and nitrate and phosphate concentrations might particularly increase downstream of major urbanized areas, especially in late summer and fall. Climate-induced hydrological impacts on water quality are expected to be locally high. For example, the nitrate increase expected with the driest projection could be as high as the impacts of direct anthropogenic pressures on the river basin (agriculture, wastewater treatment plants).

The riverine modeling platform is ready for further investigations of the cumulative and/or attenuating impacts of climate change, as well as scenarios of adaptive management practices (wastewater treatment improvements, diffuse source decreases, water regulation, etc.), in order to provide information for further management strategies in a context of changing climate.

AUTHOR CONTRIBUTIONS

VT, LO, CR, and JG conceived the project; MR, VT, MS, LO, CR, and JG contributed to the design of the study, data analysis and interpretation of data or results; MR, VT, MS, and LO conceptualized the spatialization of the hydrological model and the coupling with the biogeochemical model; MR, VT, LO, and RV identified the adequate climate products; MR and MS created the figures; MR implemented the hydrological module, ran the hydro-biogeochemical model simulations, performed output calculations, and wrote the manuscript. All authors edited, revised the text.

ACKNOWLEDGMENTS

This work was supported by Labex L-IPSL, which is funded by ANR (Grant #ANR-10-LABX-0018) and EC2CO MARICCA, which is funded by INSU/CNRS. The authors thank Thomas Noel for providing the climate model outputs. Data are available on request to the first author.

REFERENCES

- Aissa-Grouz, N., Garnier, J., Billen, G., Mercier, B., and Martinez, A. (2015). The response of river nitrification to changes in wastewater treatment (the case of the lower Seine River downstream from Paris). *Ann. Limnol. Int. J. Limnol.* 51, 351–364. doi: 10.1051/limn/2015031
- Altieri, A. H., and Gedan, K. B. (2015). Climate change and dead zones. *Glob. Change Biol.* 21, 1395–1406. doi: 10.1111/gcb.12754
- Andersen, H. E., Kronvang, B., Larsen, S. E., Hoffmann, C. C., Jensen, T. S., and Rasmussen, E. K. (2006). Climate-change impacts on hydrology and nutrients in a Danish lowland river basin. *Sci. Total Environ.* 365, 223–237. doi: 10.1016/j.scitotenv.2006.02.036
- Anglade, J., Billen, G., Garnier, J., Makridis, T., Puech, T., and Tittel, C. (2015). Nitrogen soil surface balance of organic vs conventional cash crop farming in the Seine watershed. *Agric. Syst.* 139, 82–92. doi: 10.1016/j.agry.2015.06.006

- Arnold, J. G., and Allen, P. M. (1999). Automated methods for estimating baseflow and ground water recharge from streamflow records. *J. Am. Water Resour. Assoc.* 35, 411–424. doi: 10.1111/j.1752-1688.1999.tb03599.x
- Beaufort, A., Moatar, F., Curie, F., Ducharne, A., Bustillo, V., and Thiéry, D. (2016). River temperature modelling by strahler order at the regional scale in the loire river basin, France. *River Res. Appl.* 32, 597–609. doi: 10.1002/rra.2888
- Benoit, M., Garnier, J., and Billen, G. (2015). Temperature dependence of nitrous oxide production of a luvisolic soil in batch experiments. *Process Biochem.* 50, 79–85. doi: 10.1016/j.procbio.2014.10.013
- Billen, G., and Garnier, J. (1997). The Phison River plume: coastal eutrophication in response to changes in land use and water management in the watershed. *Aquat. Microb. Ecol.* 13, 3–17. doi: 10.3354/ame013003
- Billen, G., and Garnier, J. (2007). River basin nutrient delivery to the coastal sea: assessing its potential to sustain new production of non-siliceous algae. *Mar. Chem.* 106, 148–160. doi: 10.1016/j.marchem.2006.12.017
- Billen, G., Garnier, J., Deligne, C., and Billen, C. (1999). Estimates of early-industrial inputs of nutrients to river systems: implication for coastal eutrophication. *Sci. Total Environ.* 243–244, 43–52. doi: 10.1016/S0048-9697(99)00327-7
- Billen, G., Garnier, J., and Hanset, P. (1994). Modelling phytoplankton development in whole drainage networks: the RIVERSTRAHLER Model applied to the Seine river system. *Hydrobiologia* 289, 119–137. doi: 10.1007/BF00007414
- Billen, G., Garnier, J., Némery, J., Sebilo, M., Sfratore, A., Barles, S., et al. (2007). A long-term view of nutrient transfers through the Seine river continuum. *Sci. Total Environ.* 375, 80–97. doi: 10.1016/j.scitotenv.2006.12.005
- Billen, G., Lassaletta, L., and Garnier, J. (2014). A biogeochemical view of the global agro-food system: nitrogen flows associated with protein production, consumption and trade. *Glob. Food Secur.* 3, 209–219. doi: 10.1016/j.gfs.2014.08.003
- Billen, G., Thieu, V., Garnier, J., and Silvestre, M. (2009). Modelling the N cascade in regional watersheds: the case study of the Seine, Somme and Scheldt rivers. *Agric. Ecosyst. Environ.* 133, 234–246. doi: 10.1016/j.agee.2009.04.018
- Boë, J., Terray, L., Martin, E., and Habets, F. (2009). Projected changes in components of the hydrological cycle in French river basins during the 21st century. *Water Resour. Res.* 45:W08426. doi: 10.1029/2008WR007437
- Bossard, M., Feranec, J., and Otahel, J. (2000). *CORINE land cover technical guide - Addendum 2000*. European Environment Agency Available online at: <http://www.eea.europa.eu/publications/tech40add> (Accessed July 17, 2017)
- Bourou, F., Grizzetti, B., Granlund, K., Rekolainen, S., and Bidoglio, G. (2004). Impact of climate change on the water cycle and nutrient losses in a finnish catchment. *Clim. Change* 66, 109–126. doi: 10.1023/B:CLIM.0000043147.09365.e3
- Bouwman, A. F., Bierkens, M. F. P., Griffioen, J., Hefting, M. M., Middelburg, J. J., Middelkoop, H., et al. (2013). Nutrient dynamics, transfer and retention along the aquatic continuum from land to ocean: towards integration of ecological and biogeochemical models. *Biogeosciences* 10, 1–22. doi: 10.5194/bg-10-1-2013
- Bussi, G., Janes, V., Whitehead, P. G., Dadson, S. J., and Holman, I. P. (2017). Dynamic response of land use and river nutrient concentration to long-term climatic changes. *Sci. Total Environ.* 590–591, 818–831. doi: 10.1016/j.scitotenv.2017.03.069
- Bustillo, V., Moatar, F., Ducharne, A., Thiéry, D., and Poirel, A. (2014). A multimodel comparison for assessing water temperatures under changing climate conditions via the equilibrium temperature concept: case study of the Middle Loire River, France. *Hydrol. Process.* 28, 1507–1524. doi: 10.1002/hyp.9683
- Casanueva, A., Kotlarski, S., Herrera, S., Fernández, J., Gutiérrez, J. M., Boberg, F., et al. (2016). Daily precipitation statistics in a EURO-CORDEX RCM ensemble: added value of raw and bias-corrected high-resolution simulations. *Clim. Dyn.* 47, 719–737. doi: 10.1007/s00382-015-2865-x
- Cloern, J. E. (2001). Our evolving conceptual model of the coastal eutrophication problem. *Mar. Ecol. Prog. Ser.* 210, 223–253. doi: 10.3354/meps210223
- Cloern, J. E., Abreu, P. C., Carstensen, J., Chauvaud, L., Elmgren, R., Grall, et al. (2016). Human activities and climate variability drive fast-paced change across the world's estuarine-coastal ecosystems. *Glob. Change Biol.* 22, 513–529. doi: 10.1111/gcb.13059
- Conley, D. J., Paerl, H. W., Howarth, R. W., Boesch, D. F., Seitzinger, S. P., Havens, K. E., et al. (2009). Controlling eutrophication: nitrogen and phosphorus. *Science* 123, 1014–1015. doi: 10.1126/science.1167755
- Dawson, R. N., and Murphy, K. L. (1972). The temperature dependency of biological denitrification. *Water Res.* 6, 71–83. doi: 10.1016/0043-1354(72)90174-1
- Dayon, G. (2015). *Evolution du Cycle Hydrologique Continental en France au cours des Prochaines Décennies*. Thèse de doctorat. Université de Toulouse, Université Toulouse III-Paul Sabatier.
- Desmit, X., Lacroix, L., Dulière, V., Lancelot, C., Gypens, N., Ménesguen, A., et al. (2015). *Ecosystem Models as Support to Eutrophication Management in the North Atlantic Ocean (EMoSEM)*. EMoSEM Final Report EU FP7 Seas-Era project 31/08/2015.
- Diaz, R. J., and Rosenberg, R. (2008). Spreading dead zones and consequences for marine ecosystems. *Science* 321, 926–929. doi: 10.1126/science.1156401
- Doney, S. C. (2010). The growing human footprint on coastal and open-ocean biogeochemistry. *Science* 328, 1512–1516. doi: 10.1126/science.1185198
- Ducharne, A. (2008). Importance of stream temperature to climate change impact on water quality. *Hydrol. Earth Syst. Sci.* 12, 797–810. doi: 10.5194/hess-12-797-2008
- Ducharne, A., Théry, S., Viennot, P., Ledoux, E., Gomez, E., and Déqué, M. (2003). Influence du changement climatique sur l'hydrologie du bassin de la Seine. *Vertigo - Rev. Électronique En Sci. Environ.* 4. doi: 10.4000/vertigo.3845
- EEA (2007). *CLC2006 Technical Guidelines*. Luxembourg: European Environment Agency.
- EEA (2012). *Waterbase - UWWTD: Urban Waste Water Treatment Directive*. Version of November, 2014. Available online at: <https://www.eea.europa.eu/data-and-maps/data/waterbase-uwwtd-urban-waste-water-treatment-directive>
- Erisman, J. W., Galloway, J. N., Seitzinger, S., Bleeker, A., Dise, N. B., Petrescu, A. M., et al. (2013). Consequences of human modification of the global nitrogen cycle. *Philos. Trans. R. Soc. B Biol. Sci.* 368:20130116. doi: 10.1098/rstb.2013.0116
- Gao, G., Clare, A. S., Rose, C., and Caldwell, G. S. (2017). Eutrophication and warming-driven green tides (*Ulva rigida*) are predicted to increase under future climate change scenarios. *Mar. Pollut. Bull.* 114, 439–447. doi: 10.1016/j.marpolbul.2016.10.003
- Garnier, J., Billen, G., and Cébron, A. (2007). Modelling nitrogen transformations in the lower Seine river and estuary (France): impact of wastewater release on oxygenation and N₂O emission. *Hydrobiologia* 588, 291–302. doi: 10.1007/s10750-007-0670-1
- Garnier, J., Billen, G., and Coste, M. (1995). Seasonal succession of diatoms and chlorophyceae in the drainage Network of the Seine River: observations and modeling. *Limnol. Oceanogr.* 40, 750–765. doi: 10.2307/2838310
- Garnier, J., Billen, G., Hannon, E., Fonbonne, S., Videnina, Y., and Soulie, M. (2002). Modelling the transfer and retention of nutrients in the drainage Network of the Danube River. *Estuar. Coast. Shelf Sci.* 54, 285–308. doi: 10.1006/ecss.2000.0648
- Garnier, J., Billen, G., Némery, J., and Sebilo, M. (2010). Transformations of nutrients (N, P, Si) in the turbidity maximum zone of the Seine estuary and export to the sea. *Estuar. Coast. Shelf Sci.* 90, 129–141. doi: 10.1016/j.ecss.2010.07.012
- Garnier, J., Passy, P., Thieu, V., Callens, J., Silvestre, M., and Billen, G. (2013). “Fate of nutrients in the aquatic continuum of the Seine River and its Estuary: modelling the impacts of human activity changes,” in *The Watershed Biogeochemical Dynamics at Large River-Coastal Interfaces: Linkages with Global Climate Change*, eds T. S. Bianchi, M. A. Allison, and W.-J. Cai (New York, NY: Cambridge University Press), 671.
- Henson, S. A., Beaulieu, C., and Lampitt, R. (2016). Observing climate change trends in ocean biogeochemistry: when and where. *Glob. Change Biol.* 22, 1561–1571. doi: 10.1111/gcb.13152
- Hesse, C., and Krysanova, V. (2016). Modeling climate and management change impacts on water quality and in-stream processes in the Elbe River Basin. *Water* 8:40. doi: 10.3390/w8020040
- Huntington, T. G., Balch, W. M., Aiken, G. R., Sheffield, J., Luo, L., Roessler, C. S., et al. (2016). Climate change and dissolved organic carbon export to the Gulf of Maine. *J. Geophys. Res. Biogeosci.* 121:2015JG003314. doi: 10.1002/2015JG003314

- Jacob, D., Petersen, J., Eggert, B., Alias, A., Christensen, O. B., Bouwer, L. M., et al. (2014). EURO-CORDEX: new high-resolution climate change projections for European impact research. *Reg. Environ. Change* 14, 563–578. doi: 10.1007/s10113-013-0499-2
- Justić, D., Rabalais, N. N., and Turner, R. E. (2005). Coupling between climate variability and coastal eutrophication: evidence and outlook for the northern Gulf of Mexico. *J. Sea Res.* 54, 25–35. doi: 10.1016/j.seares.2005.02.008
- Kirkby, M. J., Jones, R. J. A., Irvine, B., Gobin, A., Govers, G., Cerdan, O., et al. (2004). *Pan-European Soil Erosion Risk Assessment: The PESERA Map Version 1 October 2003, Explanation of Special Publication Ispra 2004 no. 73, S.P.I.04.73*. Available online at: <http://researchdirect.westernsydney.edu.au/islandora/object/uws%3A12030/> (Accessed July 17, 2017).
- Landelius, T., Dahlgren, P., Gollvik, S., Jansson, A., and Olsson, E. (2016). A high-resolution regional reanalysis for Europe. Part 2: 2D analysis of surface temperature, precipitation and wind. *Q. J. R. Meteorol. Soc.* 142, 2132–2142. doi: 10.1002/qj.2813
- Laverman, A. M., Canavan, R. W., Slomp, C. P., and Cappellen, P. V. (2007). Potential nitrate removal in a coastal freshwater sediment (Haringvliet Lake, The Netherlands) and response to salinization. *Water Res.* 41, 3061–3068. doi: 10.1016/j.watres.2007.04.002
- Laverman, A. M., Van Cappellen, P., Van Rotterdam-Los, D., Pallud, C., and Abell, J. (2006). Potential rates and pathways of microbial nitrate reduction in coastal sediments. *FEMS Microbiol. Ecol.* 58, 179–192. doi: 10.1111/j.1574-6941.2006.00155.x
- Nash, J. E., and Sutcliffe, J. V. (1970). River flow forecasting through conceptual models part I — A discussion of principles. *J. Hydrol.* 10, 282–290. doi: 10.1016/0022-1694(70)90255-6
- Nixon, S. W. (1995). Coastal marine eutrophication: a definition, social causes, and future concerns. *Ophelia* 41, 199–219. doi: 10.1080/00785236.1995.10422044
- Oudin, L., Andréassian, V., Perrin, C., Michel, C., and Le Moine, N. (2008). Spatial proximity, physical similarity, regression and ungaged catchments: a comparison of regionalization approaches based on 913 French catchments. *Water Resour. Res.* 44:W03413. doi: 10.1029/2007WR006240
- Oudin, L., Hervieu, F., Michel, C., Perrin, C., Andréassian, V., Anctil, F., et al. (2005). Which potential evapotranspiration input for a lumped rainfall–runoff model?: Part 2—Towards a simple and efficient potential evapotranspiration model for rainfall–runoff modelling. *J. Hydrol.* 303, 290–306. doi: 10.1016/j.jhydrol.2004.08.026
- Paerl, H. W., and Paul, V. J. (2012). Climate change: cyanobacteria. *Water Res.* 46, 1349–1363. doi: 10.1016/j.watres.2011.08.002
- Passy, P., Le Gendre, R., Garnier, J., Cugier, P., Callens, J., Paris, F., et al. (2016). Eutrophication modelling chain for improved management strategies to prevent algal blooms in the Bay of Seine. *Mar. Ecol. Prog. Ser.* 543, 107–125. doi: 10.3354/meps11533
- Perrin, C., Michel, C., and Andréassian, V. (2003). Improvement of a parsimonious model for streamflow simulation. *J. Hydrol.* 279, 275–289. doi: 10.1016/S0022-1694(03)00225-7
- Rabalais, N. N., Turner, R. E., Díaz, R. J., and Justić, D. (2009). Global change and eutrophication of coastal waters. *ICES J. Mar. Sci.* 66, 1528–1537. doi: 10.1093/icesjms/fsp047
- Raimonet, M., Cazier, T., Rocher, V., and Laverman, A. M. (2017a). Nitrifying kinetics and the persistence of nitrite in the Seine River, France. *J. Environ. Qual.* 46, 585–595. doi: 10.2134/jeq2016.06.0242
- Raimonet, M., Oudin, L., Thieu, V., Silvestre, M., Vautard, R., Rabouille, C., et al. (2017b). Evaluation of gridded meteorological datasets for hydrological modeling. *J. Hydrometeorol.* 18, 3027–3041. doi: 10.1175/JHM-D-17-0018.1
- Regnier, P., Arndt, S., Goossens, N., Volta, C., Laruelle, G. G., Lauerwald, R., et al. (2014). Modelling estuarine biogeochemical dynamics: from the local to the global scale. *Aquat. Geochem.* 19, 591–626. doi: 10.1007/s10498-013-9218-3
- Rockström, J., Steffen, W., Noone, K., Persson, A., Chapin, F. S., Lambin, E. F., et al. (2009). A safe operating space for humanity. *Nature* 461, 472–475. doi: 10.1038/461472a
- Romero, E., Garnier, J., Lassaletta, L., Billen, G., Gendreau, R. L., Riou, P., et al. (2012). Large-scale patterns of river inputs in southwestern Europe: seasonal and interannual variations and potential eutrophication effects at the coastal zone. *Biogeochemistry* 113, 481–505. doi: 10.1007/s10533-012-9778-0
- Seitzinger, S. P., Styles, R. V., Boyer, E. W., Alexander, R. B., Billen, G., Howarth, R. W., et al. (2002). “Nitrogen retention in rivers: model development and application to watersheds in the northeastern U.S.A.,” in *The Nitrogen Cycle at Regional to Global Scales*, eds. E. W. Boyer and R. W. Howarth (Dordrecht: Springer Netherlands), 199–237. doi: 10.1007/978-94-017-3405-9_6
- Strahler, A. N. (1957). Quantitative analysis of watershed geomorphology. *Eos Trans. Am. Geophys. Union* 38, 913–920. doi: 10.1029/TR038i006p00913
- Thamdrup, B., Hansen, J. W., and Jørgensen, B. B. (1998). Temperature dependence of aerobic respiration in a coastal sediment. *FEMS Microbiol. Ecol.* 25, 189–200. doi: 10.1111/j.1574-6941.1998.tb00472.x
- Tóth, G., Jones, A., and Montanarella, L. (2013). *LUCAS Topsoil Survey: Methodology, Data and Results*. Luxembourg: Publications Office of the European Union.
- Valéry, A., Andréassian, V., and Perrin, C. (2010). Regionalization of precipitation and air temperature over high-altitude catchments – learning from outliers. *Hydrol. Sci. J.* 55, 928–940. doi: 10.1080/02626667.2010.504676
- Van Cappellen, P., Dixit, S., and van Beusekom, J. (2002). Biogenic silica dissolution in the oceans: reconciling experimental and field-based dissolution rates. *Glob. Biogeochem. Cycles* 16:1075. doi: 10.1029/2001GB001431
- Vogt, J., Soille, P., de Jager, A., Rimaviciute, E., Mehl, W., Foisneau, S., et al. (2007). *A Pan-European River and Catchment Database*. Luxembourg: EC-JRC.
- Vrac, M., Drobinski, P., Merlo, A., Herrmann, M., Lavaysse, C., Li, L., et al. (2012). Dynamical and statistical downscaling of the French Mediterranean climate: uncertainty assessment. *Nat. Hazards Earth Syst. Sci.* 12, 2769–2784. doi: 10.5194/nhess-12-2769-2012
- Vrac, M., Noël, T., and Vautard, R. (2016). Bias correction of precipitation through Singularity Stochastic Removal: Because occurrences matter. *J. Geophys. Res. Atmos.* 121, 5237–5258. doi: 10.1002/2015JD024511
- Wilby, R. L., Whitehead, P. G., Wade, A. J., Butterfield, D., Davis, R. J., and Watts, G. (2006). Integrated modelling of climate change impacts on water resources and quality in a lowland catchment: river Kennet, UK. *J. Hydrol.* 330, 204–220. doi: 10.1016/j.jhydrol.2006.04.033
- Wood, S. A., Borges, H., Puddick, J., Biessy, L., Atalah, J., Hawes, I., et al. (2017). Contrasting cyanobacterial communities and microcystin concentrations in summers with extreme weather events: insights into potential effects of climate change. *Hydrobiologia* 785, 71–89. doi: 10.1007/s10750-016-2904-6

Conflict of Interest Statement: The authors declare that the research was conducted in the absence of any commercial or financial relationships that could be construed as a potential conflict of interest.

Copyright © 2018 Raimonet, Thieu, Silvestre, Oudin, Rabouille, Vautard and Garnier. This is an open-access article distributed under the terms of the Creative Commons Attribution License (CC BY). The use, distribution or reproduction in other forums is permitted, provided the original author(s) and the copyright owner are credited and that the original publication in this journal is cited, in accordance with accepted academic practice. No use, distribution or reproduction is permitted which does not comply with these terms.